Probabilistic Seismic Hazard Analysis Based on Seismic Wave Inventory

K. Tanaka
Railway Technology Research Institute, Tokyo

T. Itoi & T. Takada
The University of Tokyo, Tokyo

SUMMARY: (10 pt)
After the 1995 Kobe earthquake, strong ground motion observation network has been intensively developed in Japan. And a great amount of observed data has been accumulated. In the past study, we proposed the wave selection method based on, "Seismic Wave Inventory (SWI)", for the objective that the database can be effectively used for structural design. The ground motion data in the database is classified by their attributes such as source magnitude and distance etc. The dataset satisfying user requirement is chosen from the database by the help of SWI. In this study, the concept of SWI is extended for PSHA as well as for a design ground motion selection method corresponding to a target return period. The feature of our method is that the seismic hazard curve represented in terms of an arbitrary intensity measure can be calculated. And the ground motion set corresponding to a target return period can be easily selected from the ground motion database.

Keywords: Strong ground motion database, Selection, PSHA, Design ground motion, Return period

1. INTRODUCTION

After the 1995 Kobe earthquake, strong ground motion observation network like K-NET and KiK-net has been developed by National Research Institute for Earth Science and Disaster Prevention (NIED). And a great amount of observed data has been accumulated, especially from 2011 Tohoku earthquake and the aftershocks. These data greatly contributed to better understanding of source mechanism and earthquake damage. However, it is not well proposed that how to use the database for structural design and seismic risk assessment. On the other hand, worldwide strong ground motion database for the NGA project is open to the public at Pacific Earthquake Engineering Research center (PEER) website (Chiou *et al*., 2008). Moreover, the scheme for selection of ground motion dataset is provided. So, we can download the ground motion dataset scaled to user defined spectrum and ASCE code spectrum.

In the past study, we proposed the wave selection method based on, "Seismic Wave Inventory (SWI)", for the objective that strong ground motion database can be effectively used for structural design (Tanaka *et al*., 2009). The ground motion data in the database is classified by their attributes such as source magnitude and distance, average velocity S-wave etc. The dataset satisfying user requirement is chosen from the database by the help of SWI.

In this study, the concept of SWI is extended for probabilistic seismic hazard analysis as well as for a design ground motion selection method corresponding to a target design return period. First, we formulate the probabilistic seismic hazard analysis. The feature of our method is that an occurrence probability is assigned to each ground motion based on a probability of each earthquake occurrence. This gives uncertainty of ground motion intensity level, while the theoretical distribution (e.g. Log-normal distribution) has been employed in the conventional method. A seismic hazard curve represented by an arbitrary intensity measure can be calculated. Then, a set of design ground motions corresponding to a target return period can be obtained because each point on the hazard curve is related to the data in database.

2. WAVE INVENTORY

2.1. Overview of Wave Inventory

Figure 1 shows overview of SWI. At first, the ground motion database which contains both observed and simulated wave is constructed. The attributes which indicates a characteristic of each ground motion is linked to it. The types of attributes are source characteristics (magnitude, focal depth, source mechanism, etc.), propagation characteristics (hypocentral distance, Q-value, a structure of deep sedimentary layers, etc.), soil conditions at a site (S-wave velocity, soil density, N-value, etc.) and intensity measures (PGA, PGV, S_A, T_d, etc.). Next, these attributes are gathered to an inventory. The user requirement is represented by values of attributes. A set of ground motion which is matched to these values is selected from the database. However, there doesn't necessarily exist the data which is completely matched to these values as shown in Fig.2. The magnitude and distance of each data (black dots) are scattered around the target values, (M_j^*, X^*). So, it is necessary to set the window of each value such as ΔM_j and ΔX. M_j of selected ground motions is ranged from $M_j^*-\Delta M_j$ to $M_j^*+\Delta M_j$ and X is ranged from $X^*-\Delta X$ to $X^*+\Delta X$. These windows are determined by an amount of ground motions contained in database.

The features of SWI are the following four points. First, an estimation result is given not by a single IM level but by a time history. Efforts for ground motion estimation are comparable to an attenuation relationship because it requires only simple parameters such as magnitude and distance. Second, the types of attributes for ground motion selection can be chosen freely. The amount of prior information is different in each earthquake scenario. If an active fault has been precisely investigated, various source parameters of the fault may be set. On the other hand, if a source could not be identified in advance (background earthquakes), only rough information of the particular source such as magnitude and distance can been known. The more prior information that is available the more precise the results would be. However, input parameters of an attenuation relationship are limited to popular ones such as magnitude, distance, and source depth. So, it is difficult to freely choose input parameters according to the amount of prior information. Third feature is that the types of attributes for ground motion selection are added later. Intensity measure is used to explain a structural response and damage. The best one which can completely explain a structural damage is not existed and new knowledge is being accumulated. When a new parameter is proposed, it can be used as attributes for ground motion selection. Fourth, estimation accuracy is immediately improved by an update of database. In an attenuation relationship, a re-fitting of the model is required for the improvement of accuracy.

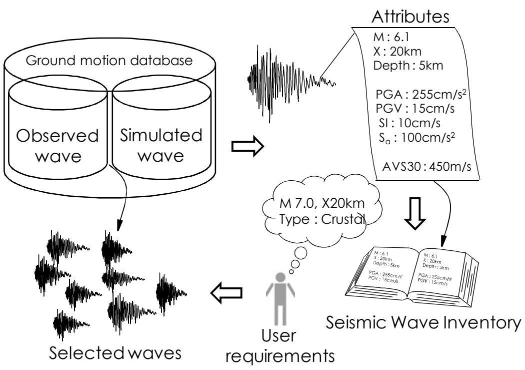

Figure 1. Overview of SWI

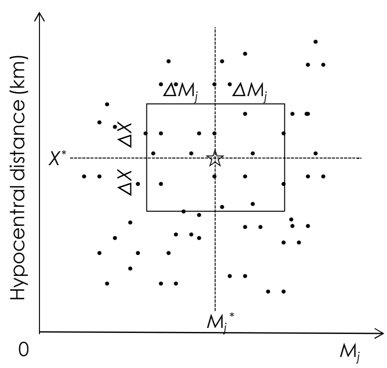

Figure 2. An area for selection of ground motions

2.2. Ground motion database

In this section, overview of ground motion database is described. In this paper, a database for only crustal earthquakes is constructed because the number of observed waves is large and the strong ground motion simulation method has been well organized as the "Recipe" (HERP, 2008). On the other hand, it is common in Japan that the ground motion simulation for subduction-zone earthquakes is performed for each scenario such as Nankai earthquake. Although the proposed method is feasible even for subduction-zone earthquakes, a discussion in this paper is limited to crustal earthquakes. Target earthquakes satisfy the following conditions that JMA magnitude (M_j) is greater than 5.0 and source depth is smaller than 25 km.

2.2.1. Observed Data

Observed data contain in database satisfy the following conditions that hypocentral distance is ranged from 5 to 100km and AVS30 (Average shear-wave velocity in the upper 30m) of observed sites is ranged from 350 to 750m/s. This soil range is almost corresponded to C class in NEHRP site class. So, selected data from database are comparable to ground motions at engineering bedrock. Further to AVS30 condition, the data strongly affected by nonlinear response of the soil are eliminated. The lower limit of hypocentral distance is decided from the lower limit of earthquake occurrence layer and from the smallest distance of collected data. EW, NS components of ground motion are regarded as independent data. Observed data are gathered from three agencies, NIED (K-NET, KiK-net), Japan Meteorological Agency (JMA) and PEER.

In this database, dataset collected from three agencies are gathered. So, it is concerned about the possibility that each dataset has different characteristics. Especially, the worldwide ground motion is contained in PEER database. Figure 3 shows mean of PGA, PGV (M_j=6.3, 6.6, 6.9) evaluated from each three datasets. The trend of three agencies are the almost same. It is confirmed that PEER dataset doesn't have a specific bias compared to dataset in Japan so database is constructed by mix of three datasets.

The characteristics of database are described here. Figure 3 shows the number of the data in each bin. The data at small distance and large magnitude bin is not enough. The data at these bins are complemented by ground motion simulation method in 2.2.2. Figure 2 shows scatter plot of M_j-distance. Figure 5 shows scatter plot of PGA and PGV. The number of the data the PGV of which is greater than 50cm/s is 17 records and the PGA of which is greater than 1000cm/s^2 is 7 records.

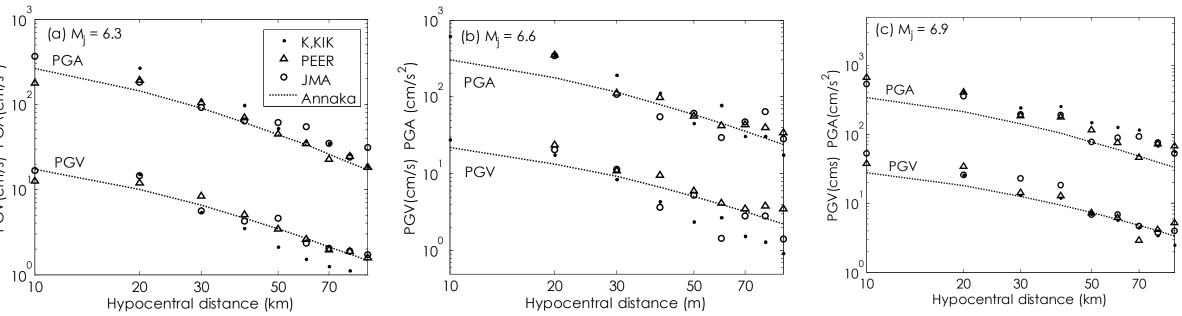

Figure 2. Attenuation relationship of PGA, PGV in 3 agencies (M_j = 6.3, 6.6, 6.9)

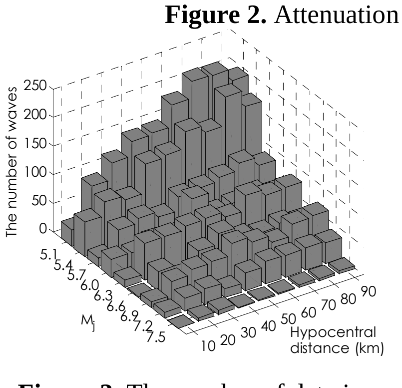

Figure 3. The number of data in each bin

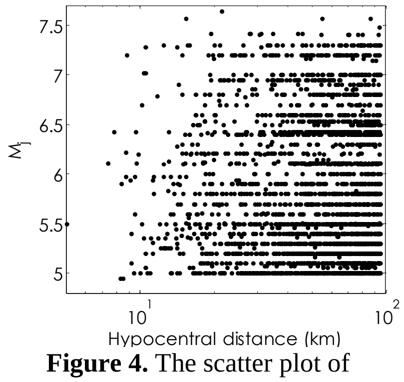

Figure 4. The scatter plot of magnitude-distance in all data

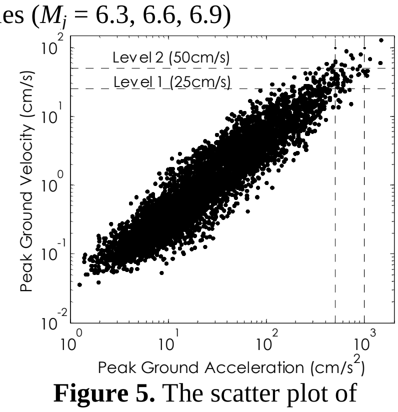

Figure 5. The scatter plot of PGA-PGV in all data

2.2.2. Simulated Data

Ground motions are calculated based on the stochastic Green's function method. The fault parameters are decided based on the "Recipe" (HERP 2008). These parameters are finally adjusted as mean trends of simulated dataset at each bin are consistent to those of observed dataset constructed in 2.2.1. Ground motions at V_s = 400m/s are calculated by the same condition as Itoi *et al.*(2009). Figure 6 shows location of receiver sites. The number of simulated data should be complemented is different for each bin, so the density of receiver sites is changed for each event. Table.1 shows the fault parameter of M_j = 6.6. Figure 7 shows the fault model arranged based on Hata *et al*. (2005), which proposes ground motion simulation method for background earthquake. The number of simulated data is 746 at 22 events and 13% of database. Figure 8 shows the comparison of intensity measure between observed and simulated data (M_j 6.6, X 20,30km). It can be observed from these figures that both trends are almost the same.

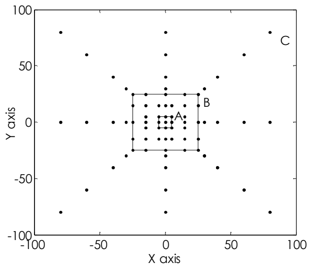

Figure 6. Location of receiver sites (A, B, C)

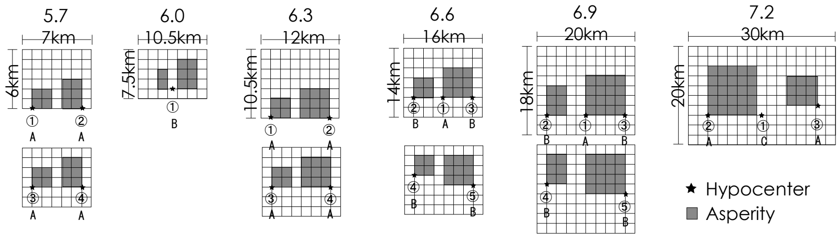

Figure 7. The fault model for each event (A, B, C in the figure show the receiver sites for each event.)

Table1. The fault parameters of M_j 6.6 (Two values in the same bin are corresponding to each 2 asperities.)

M_j	6.6	Rupture Propagation Velocity (km/s)	2.5
M_w	6.2	Asperity Area (km^2)	36, 16
Seismic Moment (N・m)	4.21×10^{18}	Asperity Area Ratio	0.23
Fault Length (km)	16	Seismic Moment of Asperity (N・m)	1.51×10^{18}, 4.47×10^{17}
Fault Width (km)	14	Stress Drop of Asperity (MPa)	13.2, 13.2
Fault Area (km^2)	224	Background Area (km^2)	172
Depth of Fault Top (km)	3	Seismic Moment of Background (N・m)	2.26×10^{18}
Dip Angle (dig)	45	Stress Drop of Background (N・m)	1.17
Density near Fault (kg/m^3)	2.8		

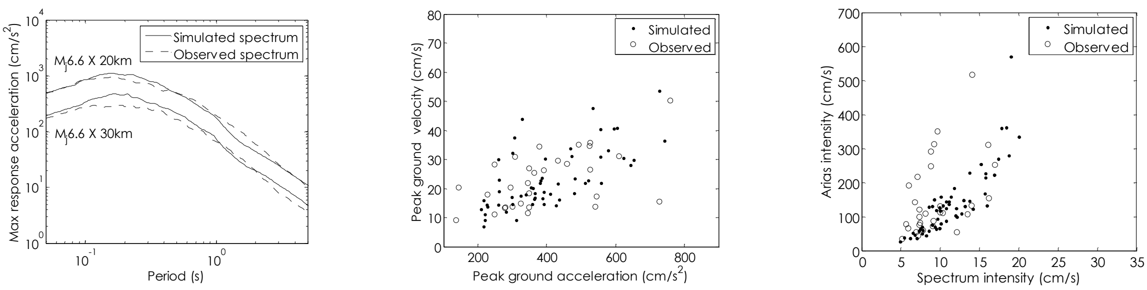

Figure 8. The comparison of intensity measures (S_A, PGA, PGV, Spectral intensity, Arias intensity) between observed and simulated data (M_j 6.6, X 20,30km)

2.2.3. Statistical characteristics of constructed database

The number of data finally contained in database is 5708. Observed data are 4962 (K-NET, KiK-net:3045, JMA:778, PEER:1139) and simulated data are 746. The largest PGA is 1467cm/s^2 and PGV is 129cm/s. Figure 9 shows the scatter plot of magnitude-distance. Figure 10 shows Log-mean PGV at each bin. Figure 11 shows the ratio that Log-mean PGV evaluated at each bin is divided by Log-mean evaluated by Annaka's attenuation relationship (Annaka *et al*., 1997). It is found that Log-mean in database is overestimated about 1.5 times at small distance and underestimated about 0.5 times at large distance compared to attenuation relationship. Figure 12 shows Log-standard deviation at each bin. Standard deviation at large magnitude bins is smaller than that at other bins

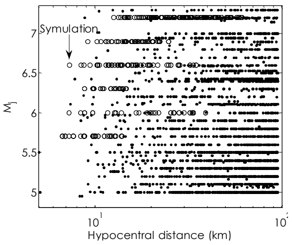

Figure 9. The scatter plot of magnitude -distance in database

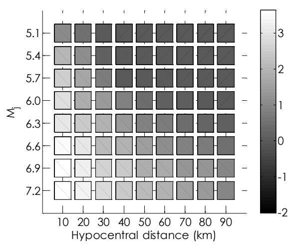

Figure 10. Log-mean of PGV at each bin

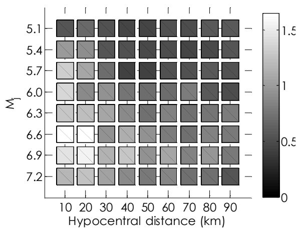

Figure 11. The ratio of Log-mean of PGV

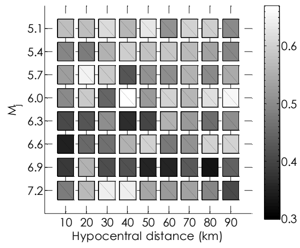

Figure 12. Log standard deviation of PGV at each bin

2.3. Application of SWI

In this section, brief application of SWI is presented. Figure 13 shows selected set of ground motions at M_j = 7.0, fault distance X_F = 15km. Figure 14 shows Response Acceleration Spectra, the mean value of which is comparable to that calculated by attenuation relationship. The window of each selection parameter is determined by a convergence of frequency distribution of intensity measure. Figure 15 and 16 show frequency distribution of PGA, PGV, the statistic (median, Log-standard deviation) of which is almost converged at ΔM_j=0.1, ΔX_F=8km. Then, it is concluded that sufficient data are selected to explain the ground motion of the target event. The mean of PGA evaluated from the distribution in Fig.15 is 307cm/s^2 and that of PGV in Fig.16 is 21.3cm/s. These values are comparable to the values evaluated by attenuation relationship. This result shows that we can gain the same information as attenuation relationship from dataset selected by SWI.

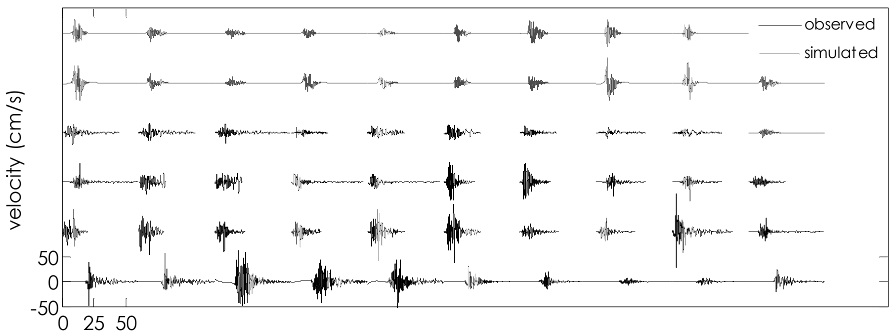

Figure 13. The set of selected ground motions at M_j 7.0, X_F 15km

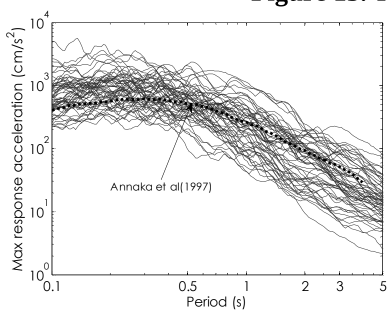

Figure 14. Response Acceleration Spectra of selected ground motions

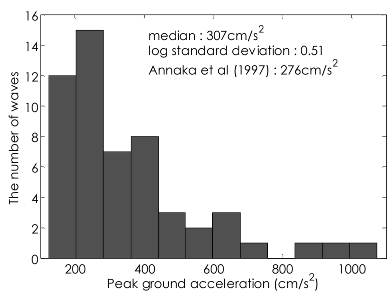

Figure 15. PGA frequency distribution of selected ground motions

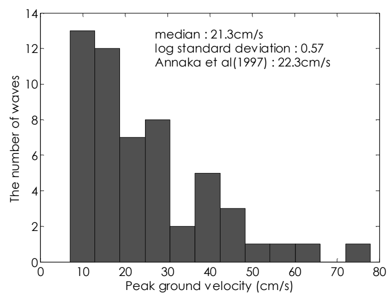

Figure 16. PGV frequency distribution of selected ground motions

3. PSHA BASED ON SWI

Probabilistic Seismic Hazard Analysis (PSHA) based on SWI is proposed. The conventional PSHA based on the empirical attenuation relationship has the following two problems, which can be solved by the proposed method.

1. A seismic hazard curve which expresses the relationships between a level of intensity measure

and its annual exceedance probability is evaluated by PSHA. In the conventional PSHA based on an attenuation relationship, a type of IM cannot be freely chosen because the types of IM fully depends on the used attenuation relationship associated with popular IMs such as PGA and PGV, S_A. So, it is difficult to flexibly change a type of IM. In the proposed method, it is possible to select a type of IM depending on the structure and the level of damage.

2. The single IM value corresponding to the exceedance probability of interest is given by the seismic hazard curve. If users require a time history of ground motion, other properties of ground motions are needed to re-produce a time history corresponding to the single value. As it has been pointed out in many papers, the image of earthquake source is lost because the result of PSHA is the one aggregated from the effects of many sources. The most popular method to solve this problem is deaggregation of hazard curve proposed by McGuire (1995). In this method a contribution rate of each seismic source can be identified and other properties of a ground motion are given from these result. In the proposed method, users don't need to simulate a time history from the single IM value because database of ground motions has been already prepared and each point on hazard curve is related to the ground motion in the database.

Figure 16 shows overview of PSHA. A simple framework of the conventional PSHA is divided by the following 4 steps. First, all seismic sources around a site are taken up and properties of earthquake sources are identified such as magnitude and occurrence probability. Next when an earthquake E_k occurs, the probability that intensity measure Y exceeds y is calculated from Eqn. 3.1.

$$P(Y > y \mid E_k) = 1 - \Phi\left(\frac{\ln y - \lambda_{E_k}}{\varsigma_{E_k}}\right) \tag{3.1}$$

Here, λ_{Ek}, ζ_{Ek} denote, respectively, Log-mean and Log-standard deviation of Y when E_k occurs. Thirdly, an exceedance probability of y in E_k, $P_k(Y>y)$, is calculated from the result of step 1 and 2. Finally, an exceedance probability of y, $P(Y>y)$, is calculated by aggregation of $P_k(Y>y)$. If these steps are repeated at all y, seismic hazard curve of Y is obtained.

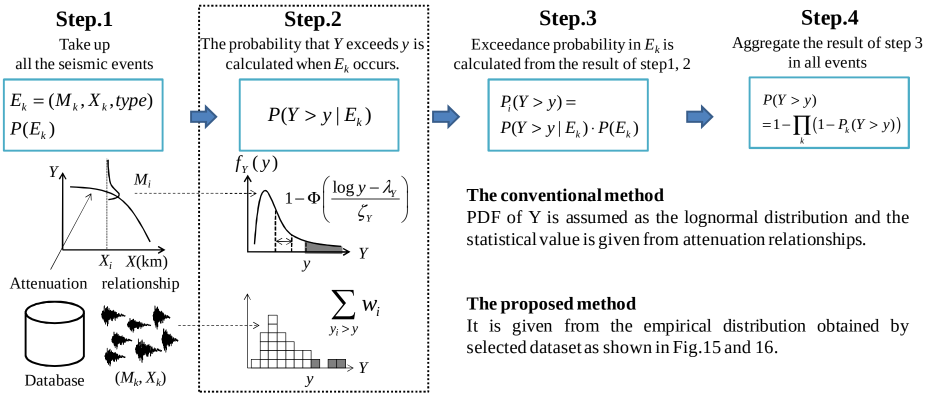

Figure 17. The framework of PSHA

The proposed method changes how to calculate $P(Y>y|E_k)$ in step 2 from the conventional PSHA. $P(Y>y|E_k)$ is calculated from an empirical distribution of Y which is estimated by selected data for E_k from the database. This distribution is the same as that shown in Figures 15 and 16. If a weight of each selected data is equal, $P(Y>y|E_k)$ is a relative rate of the data that Y exceeds y. Once, a value of IM is calculated to each data in database as attributes, it is possible to perform PSHA by any types of IM.

4. CASE STUDY OF THE PROPOSED METHOD

4.1. Overview of Case Study

In chapter 4, the proposed method is applied to the site where a source area concentrically spreads in the point of 5km in depth as shown in Fig.18. In this area, a frequency of earthquake occurrence ($4.95< M_j <7.35$, $10<X<100$km) is 1/year. b is set to 0.9. In the calculation, M_j is discretized into 8 points, 5.1, 5.4, 5.7, 6.0, 6.3, 6.6, 6.9, 7.2 and ΔM_j is set to 0.15. X is discretized into 9 points, 15, 25, 35, 45, 55, 65, 75, 85, 95km and ΔX is set to 5km.

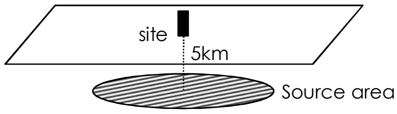

Figure 18. A seismicity around the case study site.

4.2. Theoretical Aspect of the Proposed Method

Theoretical aspect of the proposed method is described in this section. It is assumed at a case study in chapter 4 that background earthquake area exists under the site, where the occurrence model is regarded as stationary poisson process. So, theoretical model described in this paper is focused on applications for background earthquake model. The case which is assumed non-stationary occurrence model such as BTP model is discussed in Tanaka *et al*. (2011).

In background earthquake, the model of earthquake occurrence is characterized by two parameters, ν and b. ν is a frequency of earthquake occurrence and b is a slope of Gutenberg-Richter equation. ν shows a level of seismicity. b shows a relative magnitude distribution at a source area. Now, an earthquake E_{nij} occurs at a source area A_n. Magnitude is expressed by random variable M and hypocentral distance is X. In E_{nij}, a range of M is from $m_i - \Delta m$ to $m_i + \Delta m$ and that of X is from $x_j - \Delta x$ to $x_j + \Delta x$. When E_{nij} occurs, the probability that Y exceeds y in t years $P_{nij}(Y>y;t)$ is given as Eqn. 4.1.

$$P_{nij}(Y > y;t) = 1 - \exp[-\nu_{nij}(Y > y)\cdot t] \tag{4.1}$$

$\nu_{nij}(Y>y)$ is expressed as Eqn. 4.2 by ν_{nij} which denotes a frequency of earthquake E_{nij} occurrence.

$$\nu_{nij}(Y > y) = \nu_{nij}\cdot P(Y > y \mid E_{nij}) \tag{4.2}$$

ν_{nij} is expressed as Eqn. 4.3 in terms of probability density function of M and X, f_M,, f_X.

$$\begin{aligned}\nu_{nij} &= \nu_n \cdot \int_{m_i-\Delta m}^{m_i+\Delta m} f_M(m \mid A_n)dm \cdot \int_{x_j-\Delta x}^{x_j+\Delta x} f_X(x \mid A_n)dx \\ &= \nu_n \cdot P(m_i \mid A_n)\cdot P(x_j \mid A_n)\end{aligned} \tag{4.3}$$

Here, f_M is given depends on b and f_X depends on a shape of source area and geometric position between a site and a source area. ν_n denotes a frequency of earthquake occurrence at A_n. The occurrence probability of the earthquake that a magnitude range from $m_i - \Delta m$ to $m_i + \Delta m$, $P(m_i|A_n)$, is given as Eqn. 4.4.

$$P(m_i \mid A_n) = \frac{\exp[-\beta_n(m_i+\Delta m)] - \exp[-\beta_n(m_i-\Delta m)]}{\exp[-\beta_n(M_{\max}+\Delta m)] - \exp[-\beta_n(M_{\min}-\Delta m)]}, \quad \beta_n = b_n \log 10 \tag{4.4}$$

Here, b_n is b-value at source area A_n. If a source area spreads concentrically against the target site, the probability of the earthquake that a distance range from $x_j - \Delta x$ to $x_j + \Delta x$, $P(x_j|A_n)$, is given as Eqn. 4.5.

$$P(x_j \mid A_n) = \frac{4x_j\Delta x}{(X_{\max}+\Delta x)^2 - (X_{\min}-\Delta x)^2} \tag{4.5}$$

Here, $X_{\max}$, $X_{\min}$ show the maximum and minimum hypocentral distance assumed in source area A_n. When E_{nij} occurs, the probability that Y exceeds y, $P(Y>y|E_{nij})$, is expressed as Eqn. 4.6.

$$
\begin{aligned}
&P(Y>y \mid E_{nij}) = \sum_{l_{nij}\in L_{nij}} w_{l_{nij}} \\
&L_{nij} = \left\{ l_{nij} \mid y_{l_{nij}} > y, \quad l_{nij} = 1,\cdots,N(E_{nij}) \right\}
\end{aligned}
\tag{4.6}
$$

y_{lnij} denotes the value of Y of ground motion $\mathbf{g}_{lnij}$. $\mathbf{g}_{lnij}$ is the $l_{nij}{}^{th}$ ground motions selected from database for E_{nij}. The exceedance probability calculated by Eqn 4.6 is similar to that calculated by Eqn 3.1 in the conventional PSHA. In the proposed method, it's calculated by a sum of a weight of ground motion the Y value of which exceeds y as shown in Fig.17. P_{nij} $(Y>y;t)$ is expressed as Eqn. 4.7 by Eqn. 4.1, 4.2, 4.3, 4.6.

$$
P_{nij}(Y>y;t) = 1-\exp\left[-\nu_n \cdot t \cdot \sum_{l_{nij}\in L_{nij}} w_{l_{nij}} \cdot P(m_i \mid A_n)\cdot P(x_j \mid A_n)\right] \tag{4.7}
$$

Here, occurrence probability of $\mathbf{g}_{lnij}$ in t years, $P(\mathbf{g}_{lnij}; t)$, is given as Eqn. 4.8.

$$
P(\mathbf{g}_{l_{nij}};t) = 1-\exp\left[-\nu_n \cdot t \cdot w_{l_{nij}} \cdot P(m_i \mid A_n)\cdot P(x_j \mid A_n)\right] \tag{4.8}
$$

Eqn 4.7 is expressed as Eqn 4.9 using $P(\mathbf{g}_{lnij}; t)$.

$$
\begin{aligned}
P_{nij}(Y>y;t) &= 1-\prod_{l_{nij}\in L_{nij}} \exp\left[-\nu_n \cdot t \cdot w_{l_{nij}} \cdot P(m_i \mid A_n)\cdot P(x_j \mid A_n)\right] \\
&= 1-\prod_{l_{nij}\in L_{nij}} \left[1-P(\mathbf{g}_{l_{nij}};t)\right]
\end{aligned}
\tag{4.9}
$$

And the probability that Y exceeds y at A_n in t years, P_n $(Y>y;t)$, is expressed as Eqn. 4.10.

$$
\begin{aligned}
P_n(Y>y;t) &= 1-\prod_i \prod_j \left[1-P_{nij}(Y>y;t)\right] \\
&= 1-\prod_i \prod_j \prod_{l_{nij}\in L_{nij}} \left[1-P(\mathbf{g}_{l_{nij}};t)\right]
\end{aligned}
\tag{4.10}
$$

As shown in equation Eqn. 4.10, Seismic hazard curve at source area A_n can be calculated from $P(\mathbf{g}_{lnij}; t)$. And the contribution rate of $E_{n,i1,j1}$ is expressed as Eqn. 4.11.

$$
\begin{aligned}
&C_{n,i1,j1}(Y=y;t) = \frac{f_{Y,n,i1,j1}(y;t)}{\sum_i \sum_j f_{Y,n,i,j}(y;t)} \approx \frac{1-\prod_{l_{n,i1,j1}\in L''_{n,i1,j1}} \left[1-P(g_{l_{n,i1,j1}};t)\right]}{\sum_i \sum_j \left[1-\prod_{l_{nij}\in L''_{nij}} \left(1-P(g_{l_{nij}};t)\right)\right]} \\
&L''_{nij} = \left\{ l_{nij} \mid y_{l_{nij}} \in (y-\Delta y, y+\Delta y) \right\}
\end{aligned}
\tag{4.11}
$$

4.3. Results of Seismic Hazard Curve

Figures 19-21 shows seismic hazard curve evaluated by the proposed method. The 3 dot lines is calculated by the conventional method and r = 0.5, 1.0, 1.5 is multiplied to mean value of Y evaluated by attenuation relationship. The common trend shown in Fig.19 and 20 is that the curve evaluated by the proposed method meets to a dot line (r = 0.5) around small intensity level and to a dot lines (r = 1.5) around large intensity level. These results are consistent to the mean value trend of each bin which is shown in Fig.11.

The other trend can be seen from these results is that the curve falls in a staircase pattern around large intensity level. This results from 2 causes. First, there doesn't necessarily exist the data corresponding to these levels in database. In Fig.20, there is no data the PGV of which is ranged from 80 to 90cm/s so the hazard curve is parallel to *x*-axis. Second, exceedance probability of the curve is estimated discretely because a probability density function of Y is given as discrete distribution rather than continuous one. Although the curve evaluated by the proposed method is in a stair pattern at all intensity range, the stair is highlighted at a small exceedance probability. From a combination of these causes, the curve becomes like a staircase.

As described in chapter 3, a feature of the proposed method is that it is possible to evaluate the seismic hazard curve by any types of IM. Figure 21 shows CAV (Cumulative Absolute Velocity) hazard curve. Attenuation relationship of CAV is not popular in Japan. Judging from a definition of CAV, it is difficult to re-product a ground motion which has a CAV level of interest. The hazard curve can be easily evaluated by the proposed method and it is easy to select ground motion dataset because each point on the hazard curve is corresponding to the data in database.

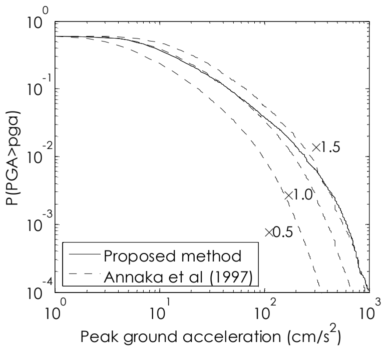

Figure 19. PGA hazard curve

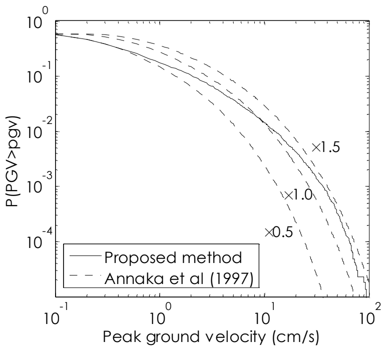

Figure 20. PGV hazard curve

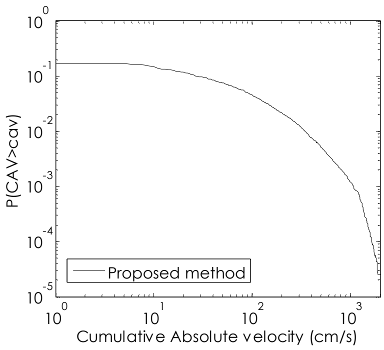

Figure 21. CAV hazard curve

4.4. Selected data corresponding to return period

In this section, dataset at return period of interest is selected. PGV is used as the type of IM. Figure 22 shows selected data at return period = 500 years. PGV_{500} is evaluated to 27.8cm/s from Fig.20. PGV of these data is ranged from 27.8-2.8 to 27.8+2.8 (p_m=10%). p_m shows a window rate of PGV for data selection. The setting method of p_m is described later. The draw position of each data in Fig.22 shows magnitude and distance of the data. These selected data has the almost same PGV but a waveform is different by magnitude and distance. The waveform at small distance has small duration time. The black line shows observed data and gray line does simulated data. Selected data at return period (5000 years, PGV_{5000} = 55.6 cm/s) are shown in Fig.23. PGV of these data is ranged from 55.6-8.3 to 55.6+ 8.3 (p_m=15%).

Figure 24 shows a variation of a distribution of contribution rate at return period (500 years) when the selection window rate p_m changes. The contribution rate at each bin is calculated from Eqn. 4.11. From these results, a convergence of a distribution is observed at p_m=10, 20%. In order to quantitatively evaluate the convergence, mean magnitude $\bar{M}_j$ and distance $\bar{X}$ of a distribution is calculated as shown in Fig.25. Judging from a convergence of $\bar{M}_j$ and $\bar{X}$, p_m is set to 10% at 100, 500, 1000 years return periods and 15% at 5000 years. Figure 26 shows the contribution distribution of two return periods, 500, 5000years.

5. CONCLUSION

In this paper, new formulation of Probabilistic Seismic Hazard Analysis based on Seismic Wave Inventory is proposed. This method solves two basic problems of the conventional method based on the attenuation relationships. First, PSHA is performed by limited types of IM such as PGA, PGV and S_A. Second, it is difficult to prepare ground motion datasets corresponding to a return period of interest. In chapter 4, a case study is shown and the validation of proposed method is examined. In the future works, the database should be expanded to the database for subduction-zone earthquakes. And the more quantative method for setting the selection window is needed.

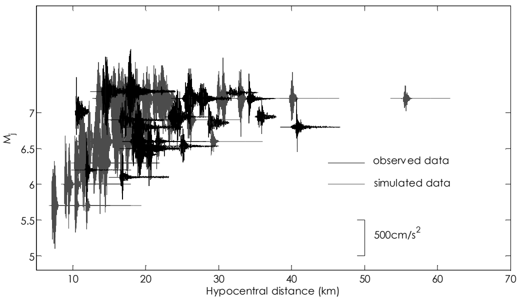

Figure 22. Selected data (500 years)

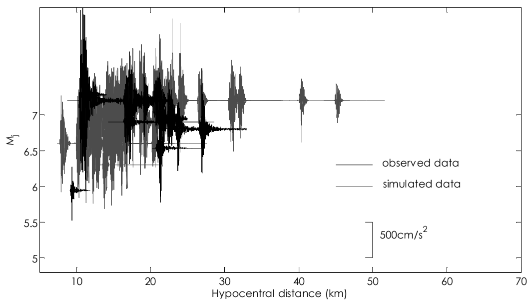

Figure 23. Selected data (5000 years)

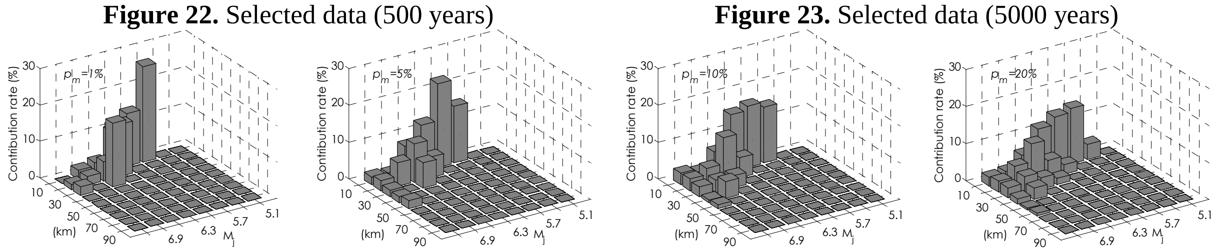

Figure 24. The distribution of contribution rate of each bin (500 years, p_m=1, 5, 10, 20%)

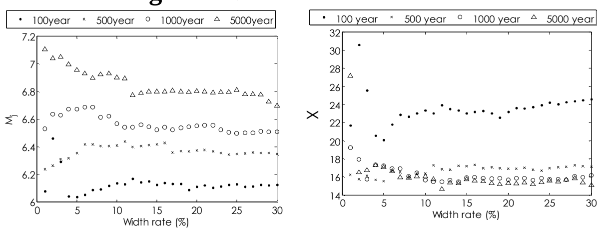

Figure 25. $\bar{M_j}$ and $\bar{X}$ at each p_m

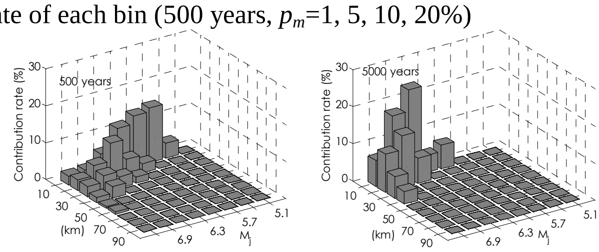

Figure 26. The distribution of contribution rate of each bin (500, 5000years)

AKCNOWLEDGEMENT

This work was supported by Grant-in-Aid for JSPS Fellows (No.22・8559). The ground motion data used in this study are provided by National Research Institute for Earth Science and Disaster Prevention, Japan Meteorological Agency, Pacific Earthquake Engineering Research Center.

REFERENCES

Annaka, T., Yamazaki, F., and Katahira, F., (1997), Proposal of attenuation equations for peak ground motion and response spectrum using JMA-87 type accelerogram, *in Proceedings of the 24th JSCE Earthquake Engineering Symposium*, 161-164.

Chiou, B., Darragh, R., Gregor, N., and Silva, W., (2008), NGA project strong-motion database, *Earthquake Spectra* **24**, 23-44.

Hata, N., Kanda, J., Dan, K., Kaneko, M., Miyakoshi, J. and Muto, T., (2005), *Proceedings of the Ninth International Conference on Structural Safety and Reliability*, 636-644.

Headquarters for Earthquake Research Promotion (2008), Strong ground motion prediction method ("Recipe") for earthquakes with specified source faults (April 11, 2008) (in Japanese)

Itoi, T., Midorikawa, S., Kito, J., Miura, M., Uchiyama, Y., and Sakamoto, S., (2009), Variability in Response Spectra of Ground Motion from Moderate Crustal Earthquake Using Stochastic Green's Function Method, *Sixth International Conference on Urban Earthquake Engineering*, 67-72

Tanaka, K., Takada, T., (2009), Empirical selection method for ground motion prediction from observed earthquake record inventory, *Journal of Structural and Construction Engineering* **646**, 2219-2225. (in Japanese)

Mcguire, R. K., (1995), Probabilistic seismic hazard analysis and design earthquake : Closing the loop, *Bulletin of the Seismological Society of America* **85:5**, 1275-1284.

Tanaka, K., Itoi, T., Takada, T., (2011), Selection of design ground motions from seismic wave inventory considering occurrence probability: proposal of simple method for probabilistic seismic hazard analysis of ground motion records, *Journal of Structural and Construction Engineering* **667**, 1591-1599. (in Japanese)